67th Annual Technical Conference Proceedings
Chicago, IL, USA May 6 – 9, 2024
https://doi.org/10.14332/svc24.proc.0067

© 2024 Society of Vacuum Coaters (www.svc.org)
all rights reserved ISSN 0737-5921
ISBN 978-1-878068-44-6

How to Measure History Dependence of Transition States during Reactive Magnetron Sputtering

Josja Van Bever[1], *Dr.* Koen Strijckmans[1], Prof. Diederik Depla[1]
[1]Department of Solid State Sciences, Ghent University, Ghent, Belgium

ABSTRACT

High quality compound coatings can be deposited by reactive magnetron sputtering. Optimal stoichiometry and properties of the produced coatings can be achieved by operating in a transition state of the reactive sputtering process [1]. This state is, however, history-dependent and varies with the previous conditions used in the coating equipment [2–4]. Moreover, the process conditions during the deposition can also drift due to long term effects [5]. A discussed example is the drift of the discharge voltage as a consequence of the deposition of an insulating coating onto the vacuum chamber walls. This example was chosen because it hindered the validation of our computational model for reactive magnetron sputtering. The development of a new probe that compensates for the observed voltage drift not only advances our understanding of the reactive process, but also fixes the chosen transition state for thin film deposition.

INTRODUCTION: CLASSICAL HYSTERESIS

Reactive magnetron sputtering is a well-established technique for producing compound thin films. Typical applications include micro-electronics [6,7], architectural glass [8,9], smart windows [10] and anti-reflective coatings [11,12]. The stoichiometry of the deposited film is crucial for these applications. Therefore, a good understanding of the production process is required.

To deposit the coating, a magnetically enhanced gas discharge is ignited between the cathode or target (consisting of the metal to incorporate in the coating) and the anode (a separate object, the chamber walls, and/or the substrate to deposit onto). The deposition of a compound coating can be achieved by the introduction of a reactive gas such as oxygen or nitrogen into the vacuum chamber which reacts with the deposited metal.

The stoichiometry and other properties of the deposited coating depend on process parameters such as the discharge voltage, current, reactive gas pressure and argon pressure [1,13,14]. A typical process curve consists of one of these parameters as a function of the reactive gas flow. Often these process curves exhibit history dependent behavior, also named hysteresis [2,15]. A schematic depiction of two hysteresis curves is shown in Figure 1 for the reactive sputter deposition of aluminum with oxygen.

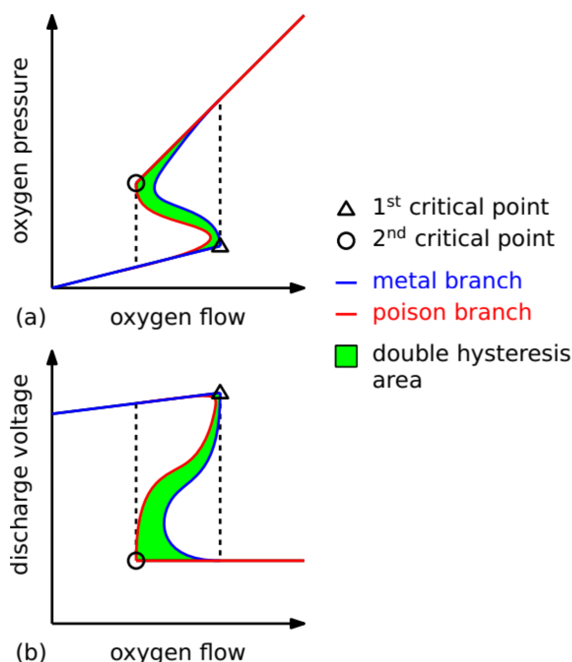

Figure 1. Schematic depiction of a hysteresis curve of the reactive sputtering of aluminum with oxygen when considering either (a) the oxygen pressure or (b) the discharge voltage as a function of the oxygen flow.

The hysteresis curves in Figure 1 can be measured in various ways. When applying flow control, the deposition condition is selected by fixing the oxygen flow and allowing the oxygen pressure and discharge voltage to stabilize. When initiating without oxygen and subsequently increasing the oxygen flow stepwise, the process first resides in metallic mode (blue path, low oxygen pressure) and abruptly switches at the first critical point (triangle) to poisoned mode (red path, high oxygen pressure). When subsequently decreasing the oxygen flow, the process returns to its initial state but only after having passed the second critical point (circle). Therefore, the oxygen pressure and discharge voltage between the flow at the first and second critical point depend on the history of the system.

67th Annual Technical Conference Proceedings
Chicago, IL, USA May 6 – 9, 2024
https://doi.org/10.14332/svc24.proc.0067

© 2024 Society of Vacuum Coaters (www.svc.org)
all rights reserved ISSN 0737-5921
ISBN 978-1-878068-44-6

Metallic and poisoned mode are characterized by a difference in the target surface condition. The target surface is metallic at low oxygen flow. The high deposition rate of aluminum results in a strong consumption of the introduced oxygen, and hence in a low oxygen pressure (Figure 1a). In poisoned mode, the target is oxidized. The oxidation occurs due to either chemisorption of oxygen onto the target surface or implantation of ionized oxygen into the target subsurface. The much lower aluminum yield from the oxidized target results in a significantly lower oxygen consumption and hence a high oxygen pressure is observed.

The discharge voltage is material dependent as it is partially defined by the ion-induced electron yield of the target [16]. In the case of aluminum, the electron yield of the oxidized surface is larger as compared to the metal, and hence the discharge voltage drops when the target gets oxidized. This explains the hysteresis curve of the discharge voltage versus the oxygen flow as depicted in Figure 1b.

HISTORY DEPENDENCE OF TRANSITION STATES

The hysteresis curves in Figure 1 exhibit a transition region (parts of the blue and red paths) that cannot be accessed by flow control. Feedback control can be used to solve this problem [1,17–21]. This approach uses one or more parameters such as the deposition rate, the discharge voltage, the reactive gas partial pressure, and an emission line to continuously control the reactive gas flow and to pin the process in transition mode.

However, even when using feedback control, the state of the process can be history dependent. When initially sputtering in metallic mode, feedback control will result in sampling of transition states on the metal branch (blue curve). In contrast, preparation of the system in poisoned mode will induce the feedback control to converge to transition states on the poison branch (red curve). When considering the oxygen pressure as a function of the oxygen flow (Figure 1), this results in a double-S shaped process curve. Hence, we will refer to this phenomenon as "double hysteresis" [2–4,22].

Double hysteresis curves are computationally predicted by a model for Reactive Sputter Deposition (the RSD-model [2,23]). This analytical model can therefore be used to understand the mechanism that causes the history dependent nature of transition states. It was found [3,22] that the separation between the transition paths is related to implanted oxygen ions. More specifically, ionized oxygen that is implanted into the target subsurface will be removed after a short time period by target erosion. Within this period, the oxygen can react with the aluminum to form aluminum oxide. However, when the erosion is too fast, the implanted oxygen is removed before reaction with the target metal. The distinction between the reacted aluminum oxide and the non-reacted oxygen ions results in a difference in oxygen pressure and discharge voltage that is observed within the process curves.

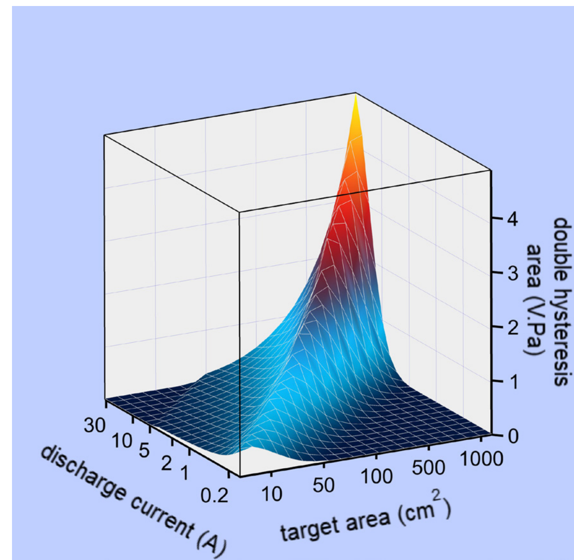

Figure 2. Evolution of the double hysteresis area (the area enclosed by the transition paths) as a function of discharge current and target area. The ridge of the slope corresponds to a constant current density of 0.025 A/cm². Data taken from [3].

The history dependence of the transition states can be further quantified by considering the area enclosed by the transition paths (green area denoted "double hysteresis area" in Figure 1). [3,22] The evolution of this area can be modeled as a function of experimental parameters such as the discharge current and the target area. This is illustrated in Figure 2. It was found [3] that (i) the double hysteresis area is maximal for a specific discharge current density (0.025 A/cm²), and (ii) when preserving a constant discharge current density, the double hysteresis area increases with the discharge current.

Observation (i) can be understood from the competition between oxide formation and target erosion. When the discharge current density is too high, all implanted oxygen is eroded from the target before reaction with the target metal. This behavior is independent of the direction the transition region is entered, i.e. from the metallic state or from the poisoned state. Hence, no difference between the transition paths is observed and the double hysteresis area is small. On the other hand, at a low discharge current density, oxide formation dominates, and all implanted oxygen has reacted regardless of the history of the target. It is only at the particular, intermediate discharge current density of 0.025 A/cm² that the formation rate of oxide and the erosion rate of implanted oxygen are comparable. In this case, the history of the target determines whether either the oxide formation or target erosion dominates. Namely, a previously metallic target exhibits a slightly higher erosion rate than a target that was previously prepared in poisoned mode. It is therefore possible that the erosion rate dominates over the oxide formation rate when entering the transition region from metallic

67th Annual Technical Conference Proceedings
Chicago, IL, USA May 6 – 9, 2024
https://doi.org/10.14332/svc24.proc.0067
© 2024 Society of Vacuum Coaters (www.svc.org)
all rights reserved ISSN 0737-5921
ISBN 978-1-878068-44-6

mode while the oxide formation rate dominates when entering the transition region from poisoned mode. In a similar fashion, observation (ii) can be understood from the increase with discharge current of both the implantation rate of oxygen ions into the target and the erosion rate of non-reacted oxygen ions from the target. In this case, an unbalance between the oxide formation rate and the erosion rate of non-reacted ions more easily results in a large difference between the transition paths. Namely, when both rates scale with the discharge current, the difference will also scale and hence larger differences in gas pressure and discharge voltage are induced.

EXPERIMENTAL VALIDATION

To validate the computational predictions, the simulated hysteresis curves are compared with experimentally obtained curves. This is not only important for the development of process understanding but also demonstrates the real impact of the historical dependence of transition states on process control.

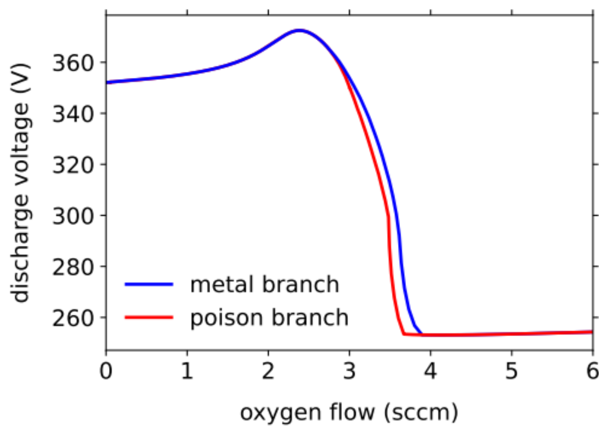

Figure 3. Simulated hysteresis curve of the discharge voltage as a function of the oxygen flow at a high pumping speed (225 l/s). The transition paths between metallic and poisoned mode are plotted separately.

Figure 3 shows an example of a simulated hysteresis curve of the reactive sputtering of aluminum with oxygen. The pumping speed was set at 225 l/s. This high pumping speed results in transition states that are stable under flow control [24].

The hysteresis curve was also measured experimentally using flow control. The process conditions were identical to the simulation input parameters. The hysteresis was obtained by initiating in metallic mode (0 sccm of oxygen) and subsequently in- and decreasing the oxygen flow stepwise with a constant time step. Two experimental curves are shown in Figure 4. The measured hysteresis curve is dependent on the time step per process point. This is undesired for comparison with a model [2,15] as the latter assumes a steady-state condition of the system. Moreover, the experiments in Figure 4 exhibit a cross-over of the transition paths near 3.2 sccm which is not retrieved in the simulation results (Figure 3).

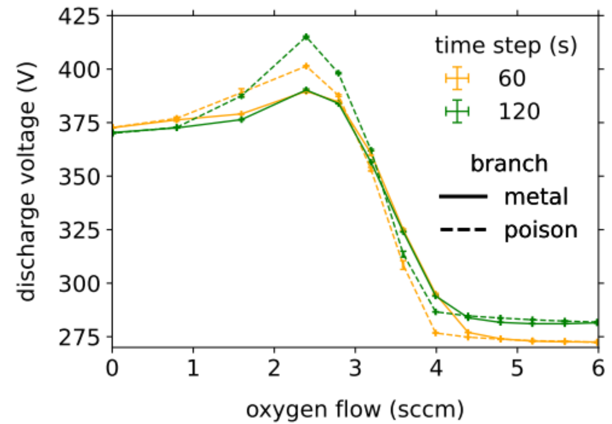

Figure 4. Measured hysteresis curves of the discharge voltage as a function of the oxygen flow. Two curves are shown that are obtained in flow control using a different time step per sampling point. The process conditions are identical to the simulation input of Figure 3.

The dependence on the time step and the disagreement with the simulations cannot be attributed to the applied process control. In fact, the high pumping speed was chosen on purpose to avoid delays specific to feedback control.

The deviations were observed to result from an offset in discharge voltage. A probe was developed that reproduces the exact same voltage offset [25]. The probe consists of a copper disk that is insulated from ground and is positioned opposite to the magnetron. A correction signal for the discharge voltage is generated with the probe as the floating potential of the copper disk during the discharge.

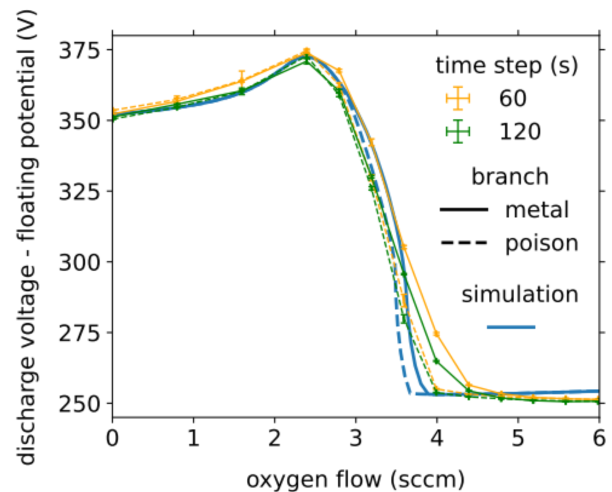

Figure 5. Measured hysteresis curves of the difference of discharge voltage and floating potential of the probe as a function of the oxygen flow. Two curves are shown that are obtained in flow control using a different time step per sampling point, together with the simulated curve. The process conditions are identical to the simulation input. Data taken from [25].

67th Annual Technical Conference Proceedings
Chicago, IL, USA May 6 – 9, 2024
https://doi.org/10.14332/svc24.proc.0067

© 2024 Society of Vacuum Coaters (www.svc.org)
all rights reserved ISSN 0737-5921
ISBN 978-1-878068-44-6

The influence of the time step on the hysteresis curves disappears to a great extent when plotting the difference of the discharge voltage and floating potential instead (Figure 5). The resulting curve exhibits only one separation in transition mode, which agrees with the simulated curve.

Both simulations (Figure 3) and experiment (Figure 5) indicate that the transition states of a reactive sputtering system are different depending on whether the target was previously in metallic or poisoned mode. This double hysteresis [2–4,22] or history dependence is attributed by the model to non-reacted implanted oxygen. We can therefore state that process control of reactive sputtering within the transition region can be history dependent due to oxygen implantation.

EXPLANATION

The deviations in the measured hysteresis curves in Figure 4 are due to a voltage shift. This voltage shift is caused by the deposition of insulating aluminum oxide onto the chamber walls. A detailed investigation is presented in [25]. Due to oxide deposition, the effective anode area decreases, and it becomes more difficult for low energy electrons to escape the discharge. Hence, the discharge voltage needs to increase to maintain the discharge current [1]. When the increased discharge voltage exceeds the voltage that can be delivered by the power supply, this results in the extinction of the discharge, which is known as the disappearing anode effect. It should be noted that the oxide layer can also act as an active source of electrons, since the secondary electron yield of aluminum oxide is much higher than for aluminum [16]. These electrons contribute to the electron density in the discharge plasma and therefore also induce a voltage shift.

The floating potential of the probe shifts to the same extent as the discharge voltage. The probe can therefore be used to correct the discharge voltage measurement. To demonstrate this use for a broader range of discharge conditions, the relationship between discharge voltage and discharge current is measured at a constant oxygen flow. The change of the discharge voltage with the discharge current is often known as an IV-characteristic (or in short IV) of the gas discharge. The measured IV-characteristics are shown in Figure 6.

Before each IV-measurement shown in Figure 6, the system was sputter cleaned for 3 to 5 min, during which any voltage shift disappears. This is because the anode gets coated with a conductive metallic layer and hence low energy electrons from the discharge can escape more easily. Next, oxygen was introduced at a flow rate of 3.0 sccm to bring the process in transition mode. By running the process in this mode over a given time (see legend of Figure 6), a predefined amount of aluminum oxide is deposited within the chamber. After the preparation time, the flow was switched to 6.0 sccm corresponding to poisoned mode and the measurement of the IV-characteristic was started within 2 min after the flow change.

The preparation time (and therefore the amount of deposited aluminum oxide) clearly affects the IV (Figure 6a) which is hence not solely defined by the discharge current (and voltage). When plotting the difference of discharge voltage and floating potential all IV-characteristics coincide except for a minor variation (Figure 6b, remark the same scale of the voltage axis). The floating potential probes can therefore be used to compensate the voltage shift for a broad range of process conditions.

The compensation of the discharge voltage shift has important practical consequences for industry. Often, chambers contain shields to diminish maintenance efforts. These shields are then sandblasted to clean the chamber wall. After this cleaning procedure, the chamber walls are in a metallic state. Hence, any deposition of insulating coatings that is done after this results in a gradual increase of the discharge voltage, but not of the difference of discharge voltage and floating potential. The floating potential probe is therefore an effective tool to monitor industrial deposition systems more efficiently.

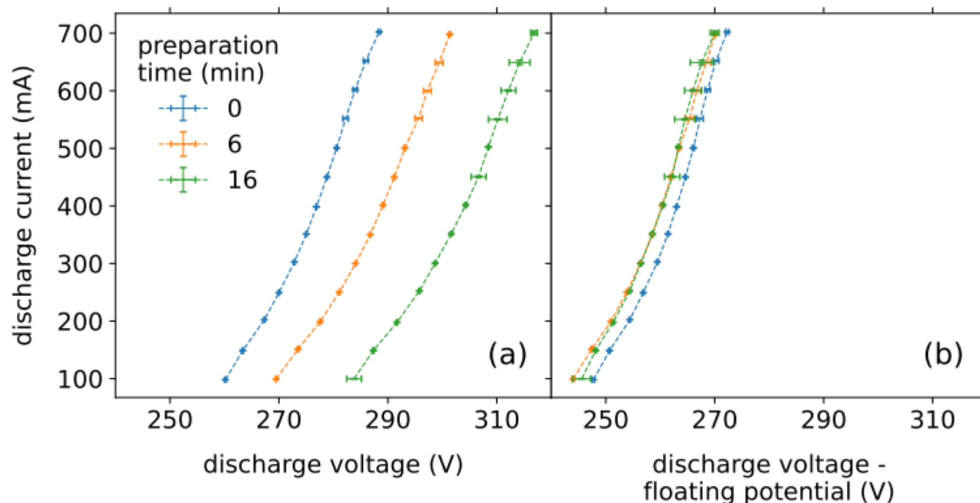

Figure 6. (a) IV-characteristics obtained at 6.0 sccm (fully poisoned mode). Each curve is prepared after a different preparation time (see legend) of the system in transition mode (3.0 sccm of oxygen). (b) Same measurements but using the difference of discharge voltage and floating potential at the planar probe instead. The data is plotted on the same scale as in figure (a) to facilitate comparison. Data taken from [25].

https://doi.org/10.14332/svc24.proc.0067
© 2024 Society of Vacuum Coaters (www.svc.org)
all rights reserved ISSN 0737-5921
ISBN 978-1-878068-44-6

CONCLUSION

During the reactive sputtering of aluminum with oxygen, insulating aluminum oxide is deposited onto the anode, which results in a shift of the discharge voltage. The voltage shift is successfully compensated by the use of a floating potential probe. The corrected hysteresis curves exhibit a single separation in transition mode, which is attributed to the presence of non-reacted implanted oxygen ions as is quantitatively predicted by the RSD-model. The floating potential probes and the model therefore prove useful for process understanding and control.

ACKNOWLEDGEMENTS

The authors wish to acknowledge Ghent University for the financial support through the project TIMERS (grant number 01J05319), the Ministry of Education, Youth and Sports of the Czech Republic for support through project LM2023039, and the "Fonds Wetenschappelijk Onderzoek" (FWO) for support through travel grant K248123N. We thank professor Stephanos Konstantinidis for borrowing the Speedflo system. The UGhent authors would like to thank Ing. Lode Tassignon for the co-development of the process control software and Stefaan Broekaert for the co-development of the home-build setup and the floating potential probe**s.** The first author would also like to thank his family and loved ones for always supporting him.

REFERENCES

[1] Sproul W.D., Christie D.J., Carter D.C. "Control of reactive sputtering processes," Thin Solid Films. 491 (1), 1–17, 2005. doi: 10.1016/j.tsf.2005.05.022.

[2] Strijckmans K., Schelfhout R., Depla D. "Tutorial: Hysteresis during the reactive magnetron sputtering process," J. Appl. Phys. 124 (24), 241101, 2018. doi: 10.1063/1.5042084.

[3] Van Bever J., Strijckmans K., Depla D. "A computational study of the double hysteresis phenomenon during reactive sputtering," J. Phys. D: Appl. Phys. 55 (35), 355302, 2022. doi: 10.1088/1361-6463/ac761c.

[4] Schelfhout R., Strijckmans K., Depla D. "The existence of a double S-shaped process curve during reactive magnetron sputtering," Appl. Phys. Lett. 109 (11), 111605, 2016. doi: 10.1063/1.4962958.

[5] Mareš P., Kadlec S., Dubau M., Marek A., Vyskočil J. "Long-term stability and disappearing anode effects during reactive DC and pulsed bipolar magnetron sputtering of Al_2O_3," Vacuum. 173, 109161, 2020. doi: 10.1016/j.vacuum.2019.109161.

[6] Licari J.J., Enlow L.R., "Thin Film Processes," Hybrid Microcircuit Technology Handbook (Second Edition), William Andrew Publishing, pp. 63–103, 1998.. doi: https://doi.org/10.1016/B978-081551423-7.50005-5.

[7] Wasa K., Kanno I., Kotera H., editors. "Handbook of Sputtering Technology (Second Edition)," William Andrew Publishing, 2012. doi: 10.1016/B978-1-4377-3483-6.00010-3.

[8] Mertin S., Hody-Le Caër V., Joly M., Mack I., Oelhafen P., Scartezzini J.L., et al. "Reactively sputtered coatings on architectural glazing for coloured active solar thermal façades," Energy and Buildings. 68, 764–70, 2014. doi: 10.1016/j.enbuild.2012.12.030.

[9] Bugaev S.P., Sochugov N.S. "Production of large-area coatings on glasses and plastics," Surface and Coatings Technology. 131 (1), 474–80, 2000. doi: 10.1016/S0257-8972(00)00843-4.

[10] Houska J. "Design and reactive magnetron sputtering of thermochromic coatings," Journal of Applied Physics. 131 (11), 110901, 2022. doi: 10.1063/5.0084792.

[11] You D., Jiang Y., Cao Y., Guo W., Tan M. "Broadband antireflective coatings in the optical communication band deposited by ion-assisted reactive magnetron sputtering," Infrared Physics & Technology. 131, 104664, 2023. doi: 10.1016/j.infrared.2023.104664.

[12] Szczyrbowski J., Bräuer G., Teschner G., Zmelty A. "Large-scale antireflective coatings on glass produced by reactive magnetron sputtering," Surface and Coatings Technology. 98 (1), 1460–6, 1998. doi: https://doi.org/10.1016/S0257-8972(97)00151-5.

[13] Mahieu S., Depla D. "Reactive sputter deposition of TiN layers: modelling the growth by characterization of particle fluxes towards the substrate," J. Phys. D: Appl. Phys. 42 (5), 053002, 2009. doi: 10.1088/0022-3727/42/5/053002.

[14] Anders A. "A structure zone diagram including plasma-based deposition and ion etching," Thin Solid Films. 518 (15), 4087–90, 2010. doi: 10.1016/j.tsf.2009.10.145.

[15] Berg S., Nyberg T. "Fundamental understanding and modeling of reactive sputtering processes," Thin Solid Films. 476 (2), 215–30, 2005. doi: 10.1016/j.tsf.2004.10.051.

[16] Depla D., Mahieu S., De Gryse R. "Magnetron sputter deposition: Linking discharge voltage with target properties," Thin Solid Films. 517 (9), 2825–39, 2009. doi: 10.1016/j.tsf.2008.11.108.

[17] Vergöhl M., Hunsche B., Malkomes N., Matthée T., Szyszka B. "Stabilization of high-deposition-rate reactive magnetron sputtering of oxides by in situ spectroscopic ellipsometry and plasma diagnostics," Journal of Vacuum Science & Technology A. 18 (4), 1709–12, 2000. doi: 10.1116/1.582412.

[18] Malkomes N., Vergöhl M. "Dynamic simulation of process control of the reactive sputter process and experimental results," Journal of Applied Physics. 89 (1), 732–9, 2001. doi: 10.1063/1.1328407.

[19] George M.A., Craves E.A., Shehab R., Knox K. "Analysis of closed loop control and sensor for a reactive sputtering drum coater," Journal of Vacuum Science & Technology A. 22 (4), 1804–9, 2004. doi: 10.1116/1.1738661.

https://doi.org/10.14332/svc24.proc.0067
© 2024 Society of Vacuum Coaters (www.svc.org)
all rights reserved
ISSN 0737-5921
ISBN 978-1-878068-44-6

[20] Woelfel C., Kockmann S., Awakowicz P., Lunze J. "Neural network based linearization and control of sputter processes," 2017 11th Asian Control Conference (ASCC) pp. 2831–6, 2017. doi: 10.1109/ASCC.2017.8287626.

[21] Woelfel C., Bockhorn D., Awakowicz P., Lunze J. "Model approximation and stabilization of reactive sputter processes," Journal of Process Control. 83, 121–8, 2019. doi: 10.1016/j.jprocont.2018.06.009.

[22] Van Bever J., Strijckmans K., Depla D. "Influence of chemisorption on the double hysteresis phenomenon during reactive sputtering," Applied Surface Science. 613, 155901, 2023. doi: 10.1016/j.apsusc.2022.155901.

[23] Strijckmans K. "Modeling the reactive magnetron sputtering process [dissertation]," Ghent University, 2015.

[24] Okamoto A., Serikawa T. "Reactive sputtering characteristics of silicon in an Ar-N_2 mixture," Thin Solid Films. 137 (1), 143–51, 1986. doi: 10.1016/0040-6090(86)90202-6.

[25] Van Bever J., Vašina P., Drevet R., Strijckmans K., Depla D. "Floating potential probes for process control during reactive magnetron sputtering," Surface & Coatings Technology. 494 (2), 131405, 2024. doi: 10.1016/j.surfcoat.2024.131405.

FOR FURTHER INFORMATION

Prof. Diederik Depla, Ghent University, www.draft.ugent.be, Diederik.Depla@UGent.be, +32-9-264-4345